Spring 2015

Selective Hydrogenation of Furfural to Furfuyl Alcohol Over Copper Magnesium Oxide

Andrew Estrup
University of Maine - Main, andrew.estrup@maine.edu

SELECTIVE HYDROGENATION OF FURFURAL TO FURFUYL ALCOHOL OVER COPPER MAGNESIUM OXIDE

by

Andrew J. Estrup

A Thesis Submitted in Partial Fulfillment
of the Requirements for a Degree with Honors
(Chemical Engineering)

The Honors College

University of Maine

May 2015

Advisory Committee:

Dr. M. Clayton Wheeler, Professor of Chemical Engineering
Dr. William J. DeSisto, Professor of Chemical Engineering
Dr. G. Peter van Walsum, Professor of Chemical Engineering
Dr. Sarah Harlan-Haughey, CLAS-Honors Preceptor of English
Dr. François G. Amar, Professor of Chemistry, Honors College Dean

Abstract

Furfural is a byproduct of biomass hydrolysis and novel means of utilizing this platform chemical are at the forefront of biofuel research. This project investigated many of the various and viable means of catalytic upgrading of furfural to other value-added chemicals, before ultimately exploring the conversion of furfural to furfuryl alcohol over a copper catalyst on a magnesium oxide support. Reasonable reaction conditions, mechanisms, and catalysts for the conversion of furfural to various products and platform chemicals exist, but no circumstance represents an obviously preferred method. The objective of this research project was to design and conduct experiments that characterize this catalyst and qualify its applicability for the selective hydrogenation of furfural to furfuryl alcohol. The catalyst was explored in terms of its conversion of furfural, selectivity to furfuryl alcohol, BET-surface area, reaction rate, and performance over time.

It was found that the catalyst performs very well for the first five hours of reaction time with furfural conversion averaging 94% with selectivity of furfuryl alcohol around 75%. But, issues arose beyond the first few hours and the reaction rate dropped by as much as 75% over 26 hours as the catalyst deactivated. There was also a reaction of furfural on the surface of the catalyst led to plugging of the reactor after approximately 20 hours.

This project is very relevant to the field of chemical engineering and biofuel research. As biofuel production increases, so will the production of furfural, and finding ways to utilize this chemical in both an economical and environmentally friendly manner will greatly impact the growth and relevance of biofuels in the upcoming years.

Acknowledgements

I would like to take this space to thank several individuals who without their help this project simply would not have been completed. I'd like to thank: Professor Wheeler for his support and guidance, even during the times I may not have deserved it. I'd like to thank Nick Hill, who whenever I seemed to have found what I perceived as an insurmountable obstacle, Nick was there to help me alleviate the problem. I'd like to thank Brian Frederick who took the time to meticulously train me on the GC-FID and Micromeritics equipment, which again, without his help this project would have deflated exactly when I most needed to crank up my work rate. I'd like to thank the Forest Byproducts Research Institute (FBRI) group members who gave feedback on my presentations and who taught me a great deal over the course of the year about a plethora of biofuel related topics. I'd like to thank Professor DeSisto for his help with my preliminary calculations for the synthesis of the co-precipitated catalyst, which proved to be the kick start to the actual lab work of this research project. I'd like to thank Professor Harlan-Haughey and Professor Amar who convinced me back in September to stick it out and finish honors, as well as Professor van Walsum for his willingness to join my thesis committee. Also, I'd like to thank the Charlie Slavin Research Fund for the purchases of chemicals required for the synthesis of the catalyst.

Table of Contents

Table of Tables

Table of Figures

1. INTRODUCTION

The effort to establish sustainable industrial practices reaches beyond our dependence on fossil fuels for their direct energy usage, but also to discover and implement replacements for fossil fuel-based organics in the products of chemicals, solvents, plastics, resins, and other widely manufactured items.[1] To take this step away from fossil fuel dependency, a versatile and renewable platform chemical will be required, and furfural has the makings to be just that as it is capable of aiding in the production of a diverse array of solvents and other various value-added chemicals. This thesis studies furfural and the furan derivatives that can be produced via its catalytic hydrogenation and further explores one reactant pathway and catalyst in the laboratory.

2. FURFURAL PROPERTIES & PRODUCTION

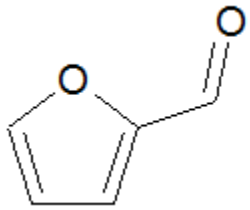

Figure 1: Chemical structure of furfural

Furfural contains a heteroaromatic furan ring with a reactive aldehyde functional group. Its molecular formula is $C_5H_4O_2$, and a few physical properties include: molecular weight of 96.08 g/mol, boiling point of 161.7°C, and minimal solubility in water, 8.3 weight percent.[1] It was first isolated in 1832 by the German chemist Johann Wolfgang Döbereiner when he noticed an oily byproduct during his synthesis of formic acid.[2] Furfural is a biobased alternative for the production of a diverse array of chemicals such

as fertilizers, paints, antacids, and plastics, and is considered one of the most promising chemicals for sustainable production of fuels and chemicals for this century.[3]

Furfural possesses physical properties that allow it to work very well as a selective extractant for uses such as removing aromatics from lubricating oils to improve the relationship of viscosity with temperature; to remove aromatics from diesel fuels to improve ignition properties; and to form cross-linked polymers.[1] Furfural is produced from five carbon sugars, mainly xylose, but also arabinose, that can be obtained from hemicellulose biomass.

Furfural is produced by the hydrolysis of hemicellulose into monomeric pentoses, such as xylose and arabinose, which go through acid-catalyzed dehydration into furfural.[1] The first means of industrial production of furfural was designed by the Quaker Oats Company; they used batch reactors at 443-458K with aqueous sulfuric acid to achieve furfural yields of nearly 50%.[1] Various researchers have studied the use of catalysts in the conversion of xylose to furfural and achieved conversions as high as 75% when utilizing mineral acids.[4]

Another method of furfural production that has gained footing is the Biofine Process, which takes biomass feedstocks to create biofuels and various value-added chemicals. The main product of the Biofine Process is levulinic acid with formic acid and furfural considered secondary prododucts.[2] Levulinic acid is also a potent platform chemical, but wide scale, industrial, and profitable uses of furfural warrant more attention for improvement.

3. POTENTIAL PRODUCTS

There are many pathways and products for the catalytic upgrading of furfural such as 2-methylfuran (MF), methyltetrahydrofuran (MTHF), tetrahydrofuran (THF), tetrahydrofurfuryl alcohol (THFA), furan, and furfuryl alcohol (FA) to name the more viable possibilities.

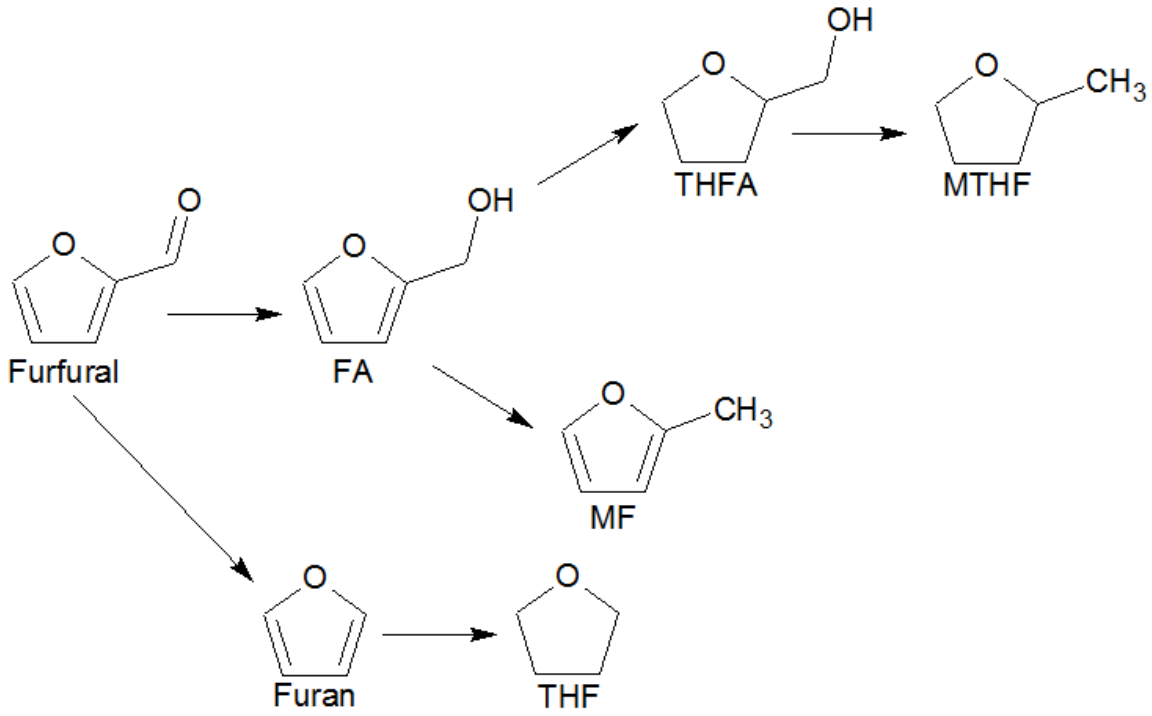

Figure 2: Furfural and the potential products considered during this research: methyltetrahydrofuran (MTHF), tetrahydrofuran (THF), tetrahydrofurfuryl alcohol (THFA), furan, and furfuryl alcohol (FA)

MF has chemical properties that give it merit as a solvent and a biofuel component that can me mixed with gasoline due to its high octane number and insolubility with water.[5] MF can be produced by the hydrogenolysis of FA. The production of MF tends to deactivate catalysts and for its production to be economically viable impeding the deactivation while promoting regeneration of the catalyst would be the main focus of further research.[1]

The two most common pathways to produce MTHF are hydrogenation through levulinic acid and hydrogenation of MF. Some of the main uses for MTHF include use as a specialty solvent, electrolyte formulation for secondary lithium electrodes[6] and as a component in alternative fuels.[7]

Decarbonylation of furfural at high temperatures produces furan through the loss of CO, and as such can be produced as a side reaction when furfural undergoes hydrogenation. High temperatures (300 to 500°C) can cause the furan ring to open and lead to the production of heavy products, which can leave carbon deposits on the catalyst causing it to deactivate.[8]

Furan can be further hydrogenated to THF, another value-added downstream product of furfural. THF is attractive for its versatility as a solvent and can be utilized in several chromatographic techniques, and to produce spandex fibers and polyurethane elastomers.[9] The hydrogenation of furfural to THF is often carried out with a Ni catalyst over a Pd support, but this approach faces challenges due to the coking that occurs, which leads to deactivation of the catalyst as the coke layer builds on its surface.[1]

THFA is soluble with water and is used as a green solvent in agricultural applications, printing inks, as well as for electronic and industrial cleaners.[1] The most common pathway to THFA is the conversion of furfural to FA over a Cu-Cr catalyst followed by the conversion of FA to THFA over a Pd/C catalyst.[10] There has been less success in creating a direct means of conversion from furfural to THFA, and as such an environmentally friendly and economically feasible conversion of furfural to FA, would benefit the production of THFA.

Each of these chemicals and the pathways of formation warrant further research. They all pose realistic applications as biomass based fossil fuel alternatives that can be used diversely across pharmaceutical, manufacturing, and fuel industries. For the purpose of this research, FA has been chosen for further study with an emphasis on understanding the catalyst. Enhancing and better understanding the catalytic conversion of furfural to FA is invaluable not only for the production of FA, but for the products that can be produced from FA such as MF, furan, THF, and THFA.

4. FURFURAL ALCOHOL PRODUCTION & CATALYSTS

FA is the most common value-added product utilizing furfural as a reactant; it is estimated that 62% of the globally produced furfural is converted to FA,[1] though as seen above much of that conversion occurs with FA as an intermediate. FA is valuable as a monomer for crosslinked-polymers to produce furan resins, which are often used for foundry binders.[2] These resins have excellent chemical, thermal, and mechanical properties, while having the capability of resisting corrosion.[11] According to Alibaba, Hongye Holding Group sells furfural at 98.5% purity for $1350 per metric ton,[12] while the same company sells FA at 98% purity for $1750.[13]

The commercial conversion of furfural to FA for many years was conducted over a Cu-Cr catalyst with an actual yield over 96% of the theoretical yield of FA at 175°C with no effect on the furan ring, though at 250°C hydrogenation would begin to occur on the furan ring.[1] Despite the high yield associated with the Cu-Cr catalyst, it was not ideal due to the presence of Cr_2O_3 (chromium oxide), which is a severe environmental pollutant.[14] There have been many studies on the catalytic conversion of furfural to FA

with varying levels of furfural conversion and FA selectivity. The catalyst and support for this conversion each play a pivotal role as selective hydrogenation of the carbonyl group to an alcohol is necessary without affecting the carbon-carbon double bonds of the furan ring. The following is an exploration of a few promising catalysts and their associated reaction conditions.

One study that examined the effect of Cu and Ni catalysts on the vapor phase hydrogenation of furfural at 10 bar H_2 and reaction temperatures of 220°C and 300°C with a CuNi catalyst on a MgAlO support was conducted by Xu et al.[14] During this experiment the Cu and Ni loadings were altered from 0 to 11.2 mole percent and 0 to 4.7 mole percent, respectively. The highest conversion of furfural, 93.2%, and selectivity of FA, 89.2%, occurred at 300°C with a Cu loading of 11.2% and a Nickel loading of 4.7%.[14]

An experiment that further examined the role of Cu catalysts in the conversion of furfural to FA was conducted by Sitthisa et al. where they examined the catalytic influence on furfural with Cu, Pd, and Ni catalysts supported on SiO_2 at 230°C and 1 atm H_2.[15] Each reaction underwent about 75% conversion of furfural. The Cu catalyst caused no hydrogenation of the furan ring and thus led dominantly to FA (98%) with small amounts of MF (2%). Pd led mostly to furan (60%) with some THF (20%) and FA (14%), and Ni led to hydrogenation of the furan ring, as well as opening of the ring and thus products such as butanal, butanol, and butane. The Ni catalyst created the most dispersed products with 32% hydrogenation, 43% decarbonylation, and 25% ring opening. This experiment further supported the claim found across literature that Cu is preferred for the selective hydrogenation of the carbonyl group of furfural. Copper is the

main catalytic active component in many of the catalysts for the hydrogenation of furfural,[14] and this is readily seen when one examines the hydrogenation pathways from furfural to FA. The catalytic centers for the furfural hydrogenation are predominantly Cu^0 species that were reduced from Cu^{2+}.[14]

Nagaraja et al. conducted vapor phase hydrogenation of furfural to FA at 180°C and 1 atm H_2 with co-precipitated Cu/MgO catalysts with Cu loadings varying from 5.2-79.8 weight percent.[16] In an earlier experiment, Nagaraja et al. analyzed and compared three catalyst preparation methods: co-precipitation, impregnation, and solid-solid wetting.[17] Their findings were that the co-precipitated catalyst had the highest BET-surface area and largest Cu-dispersion, while also having the smallest Cu particle size. These three metrics are closely related as the increased surface area of the co-precipitated catalyst occurred as the MgO surface was covered with a greater number of smaller Cu particles. The authors believe that the interaction of the Cu particles and the oxygen vacancies on the MgO surface may have aided in the larger surface area of the co-precipitated catalyst.[17] Likewise, the large number of Cu^0 sites on the surface of the co-precipitated catalyst led to a large yield of FA from furfural due to the highly active catalytic hydrogenation.[17] During this experiment the hydrogenation converted 98% of the furfural with a selectivity of 98% to FA without experiencing any catalytic deactivation over the course of the five hour experiment. Further exploration of the catalytic performance should be conducted to better understand the functioning of the catalyst. Conducting experiments with less catalyst and or for longer experimental times will see under what circumstances that catalyst begins to deactivate.

Thermodynamically, carbon-carbon double bond hydrogenation occurs more readily than hydrogenation of a carbonyl group, and the Cu particle size sterically prevents the carbon-carbon double bond hydrogenation, thus favoring selectivity towards FA.[16] Some of the main influences on the hydrogenation of furfural to FA are: metal support interactions with partially reducible supports, electronic and steric influence of the support, morphology of the metal particles, selective poisoning, effect of pressure, and steric effects of substituents at the conjugated double bond.[17]

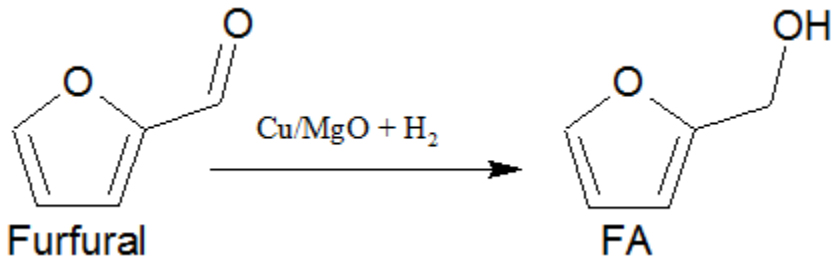

Figure 3: Reaction pathway for vapor phase hydrogenation of furfural to furfuryl alcohol over Cu/MgO

Ultimately there are many viable reaction pathways starting with furfural, but due to the flexible and wide uses of FA as a product and intermediate, the study of the catalytic hydrogenation of furfural to FA was chosen for further exploration (see Figure 3). Of the many studied catalysts, the co-precipitated Cu/MgO catalyst was chosen due to its high selectivity to FA and conversion of furfural. The emphasis of these experiments will be on further understanding the catalytic performance through metrics such as conversion and catalytic activity versus time, while examining the reaction rates from the observed performance of the catalyst over time.

Table 1: Summary of Catalyst Selection Parameters

Catalyst	Researcher	Conversion	Selectivity	Temperature (°C)	Pressure H_2	Drawbacks
Cu-Cr	Industrial Standard	53	51.9	260	1 bar	Cr_2O_3
Pd/SiO_2	Sitthisa & Resasco	69	10	230	1 atm	Low Selecvivity
Ni/SiO_2	Sitthisa & Resasco	84	31.9	210	1 atm	Ring Opening
Cu/SiO_2	Sitthisa & Resasco	77	71	270	1 atm	Adequate Conversion & Selectivity
$Cu_{11.2}Ni_{2.4}$-MgAlO	Xu & Huang	93.2	89.2	300	10 bar	Batch Reactor
Cu/MgO	Nagaraja & Rao	98	98	180	1 atm	5 Hour Experiment

5. EXPERIMENTAL METHODS

As mentioned above, the motivation of this research project was to further characterize the performance, with an emphasis on time, of the co-precipitated copper-magnesium oxide catalyst as prepared by Nagaraja & Rao (N&R). To accomplish this objective several analytical methods were of merit to be employed, and as such specific lab and equipment training were required. Some of the required instruments and analytical methods required for this research project were co-precipitated catalyst preparation, BET-surface area calculation, use of a trickle bed reactor for vapor phase hydrogenation, gas chromatograph-flame ionized detector (GC-FID) for quantitative product composition analysis. Some other methods that would have been valuable are elemental analysis, to determine the exact Cu loading of the catalyst and N_2O pulse

chemisorption to determine the number of Cu surface sites to calculate the turnover frequency.

Catalyst Co-precipitation

The first experimental step of this research was the co-precipitation of the Cu/MgO catalyst. The catalyst was prepared as follows:

1 M solutions of magnesium nitrate ($Mg(NO_3)_2$), copper nitrate ($Cu(NO_3)_2$), and potassium carbonate (K_2CO_3) were prepared from hydrates and an anhydrous salt obtained from Fischer Scientific. Calculations were made to yield 10 grams of Cu/MgO (See Table A-1). 25.2 mL $Cu(NO_3)_2$ was added with 208.5 mL $Mg(NO_3)_2$ to a 1000 mL beaker. K_2CO_3 was added slowly in increments of 5 mL with constant acidity monitoring with pH paper tests. After 350 mL of K_2CO_3 was added the solution was at a pH of 9.0. The simultaneous reactions taking place during this co-precipitation were the conversion of copper and magnesium nitrates to copper and magnesium carbonates, which can be seen in equations 1 and 2:

$$Cu(NO_3)_2 + K_2CO_3 \rightarrow CuCO_3 + 2KNO_3^- \quad (1)$$

$$Mg(NO_3)_2 + K_2CO_3 \rightarrow MgCO_3 + 2KNO_3^- \quad (2)$$

At this point the solution was a thick slurry, which was rinsed with 250 mL of distilled H_2O using a Buchner vacuum funnel and medium (particle size retention of 0.005-0.01 mm) porosity filter paper. The light blue putty was then placed in a crucible and dried in a Thermodyne 4800 Furnace at 120°C for 15 hours and then calcined in air for 4 hours at 450°C. The calcination of the magnesium and copper carbonates resulted in magnesium and copper oxides, and according to N&R[16] should have resulted in CuO particles supported on MgO. This powder was a light brownish/charcoal color, and as CuO is

black and MgO this color mix gives some indication that the two compounds are present. This reaction can be seen in equation 3:

$$MgCO_3 + CuCO_3 \xrightarrow{450°C\ in\ air} CuO + MgO + 2O_2 \qquad (3)$$

After the 4 hours of calcination the catalyst was ready for reduction and use. Once packed in the reactor the catalyst was heated to 250°C with hydrogen to reduce the copper oxide to Cu^0 species, which can be seen in reaction 4:

$$CuO + MgO \xrightarrow{250°C\ in\ H_2} Cu^0 + MgO + H_2O \qquad (4)$$

BET-Surface Area & Pore Size Distribution

BET-surface area is a measurement of the surface area of a catalyst per unit mass, and its name is derived from the individuals who created it, Brunauer, Emmett, and Teller. The theory works by monitoring equilibrium partial pressures of most commonly N_2 gas as it adsorbs on the surface of the material right at the boiling point of N_2. The Micromeritrics ASAP 2020 Surface Area and Porosity Analyzer measures the pressure of the room, the N_2 gas equilibrium pressure, and the volume of N_2 absorbed. The following equations are then used to calculate the volume of N_2 absorbed on the catalyst (Equation 5) before calculating the BET-Surface Area (Equation 6)[18].

$$V_m = V_a * \frac{(P_0 - P)}{P_0} \qquad (5)$$

Where:

V_m = the volume of gas adsorbed when the entire surface is covered with a monomolecular layer (cm^3)
V_a = volume of gas adsorbed at P (cm^3)
P_0 = N_2 saturation vapor pressure (mmHg)
P = N_2 vapor pressure (mmHg)

Once V_m is known the specific BET-surface area can be calculated by using equation 6:

$$SA = \frac{V_m * \sigma * N_A}{m * V_0} \qquad (6)$$

Where:

SA = BET-surface area (m^2/g)
V_m = volume of gas adsorbed when the entire surface is covered with a monomolecular layer (m^3)
σ = area of surface occupied by single adsorbed N_2 molecule (m^2)
N_a = Avogadro constant ($6.023*10^{23}$ molecules/mole)
m = mass of the adsorbing sample (g)
V_0 = molar volume of gas at standard temperature and pressure (m^3)

Now the average BET-surface area is calculated over the relative pressures (P/P_0) from 0.05 to 0.20.

BET-surface area was the only analytical technique employed for comparison with N&R's catalyst. The setup involves weighing a small mass of catalyst in a sample tube. The tube is then placed in the Micromeritics ASAP 2020 to degas at 250°C for 4 hours to remove any water left in the catalyst's pores and to get the tube at vacuum conditions. The tube is then moved to another part of the machine with a gas chamber above it and insulated. The free space of the tube is then determined by filling the chamber above the sample tube with known volume and pressure of He gas, then the seal frit on top of the sample tube allows He to fill the tube and come to equilibrium and the pressure change for the space above the tube allows the calculation for free space. The He gas is then removed and N_2 gas is pumped into the sample tube incrementally, allowing time for the system to come to an equilibrium pressure while monitoring the absorbed amount of N_2 at various pressures ranging from 0 to 1atm.

The N_2 adsorption results were used to estimate the pore size distribution of the catalyst. This is another valuable characterization metric as increasingly porous catalysts tend to have larger surface areas and thus more active sites. The same isotherm that is

calculated for the BET-surface area is considered here, but this time the focus is on the desorption curve. At each equilibrium pressure there is a measured amount of N_2 that desorbs from the pores, based on the pressure, each pressure corresponds to a pore size diameter based on the Kelvin Equation, and the amount desorbed indicates the relative amount of pores at that particle diameter.[18]

Reactor System

The vapor phase hydrogenation of furfural to FA was conducted in a trickle bed reactor (see FIGURE 4).

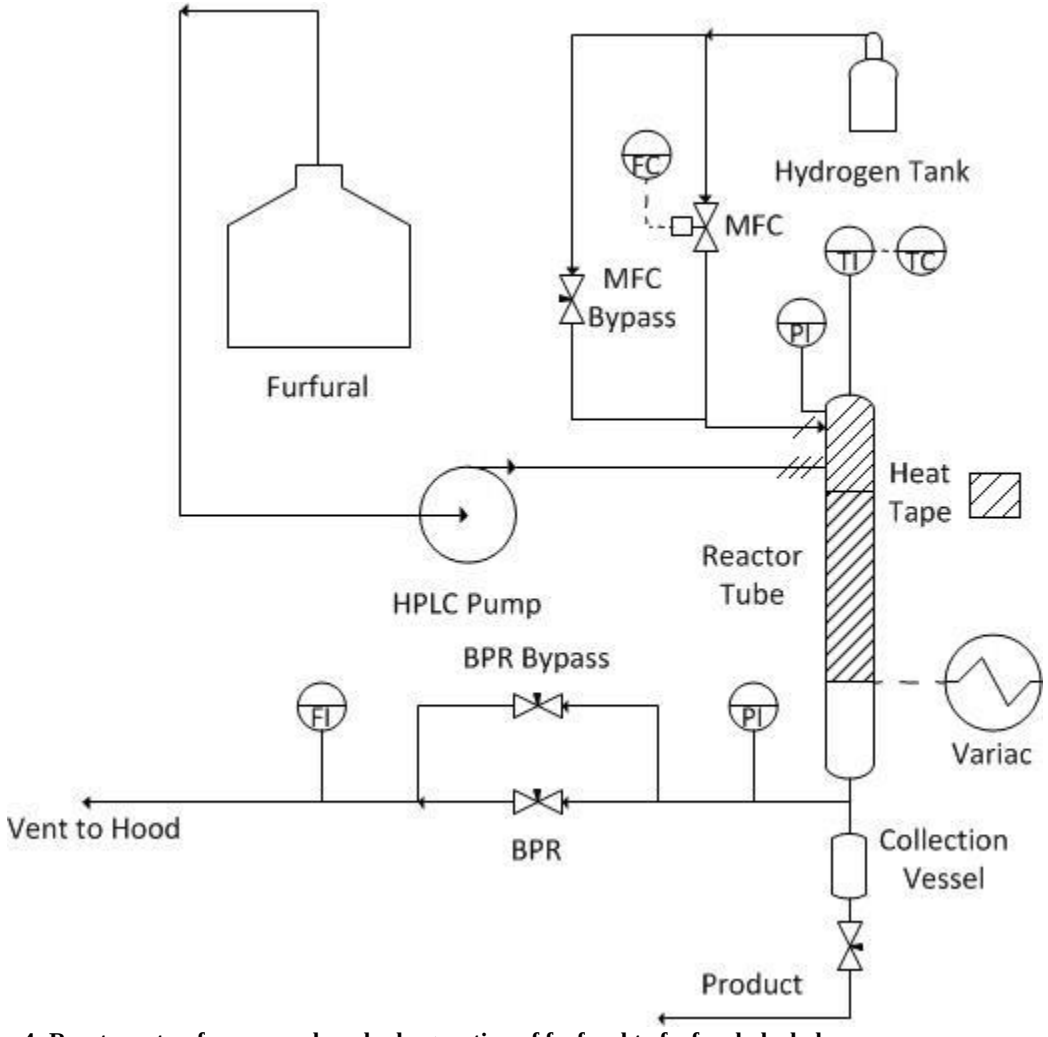

Figure 4: Reactor setup for vapor phase hydrogenation of furfural to furfuryl alcohol

Furfural was contained in a 100 mL glass storage bottle with tubing connecting it to a Scientific Systems Inc. Series III HPLC pump, as was 20% Isopropyl Alcohol (IPA) by volume, which functions as a lubricating fluid for the pump. The furfural was pumped to the top of the trickle bed reactor tube with a flow rate controlled by the HPLC pump. The hydrogen was fed from a secured storage tank through a MKS Instruments Type 247 Four Channel Mass Flow Controller (MFC). The hydrogen and furfural are fed through a 0.25" reactor tube that has an internal diameter of 0.18" and a length of 22.6". The reactor tube was packed with quartz wool above and below the catalyst (see Figure 5). The reactor tube, furfural inlet, and fittings above the hydrogen and furfural inlets were all wrapped with heat tape, which was powered by a Staco Energy 120V variable autotransformer (Variac), and this heat tape was insulated with a thin insulation and tinfoil. Temperature within the reactor was monitored by a thermocouple that was attached to a Micromega Autotune PID Temperature Controller. Temperature was monitored to ensure that the hydrogenation took place in the vapor phase. Once the vapor mixture passed through the reactor, the condensable vapors cooled and were collected as liquid products in the 100 mL sample collection vessel. The H_2 flowed through the back pressure regulator (BPR), which moderated the pressure of the system, which for all these reactions was 15 psig. The H_2 gas then passed through a rotameter before being vented through a hood to the atmosphere.

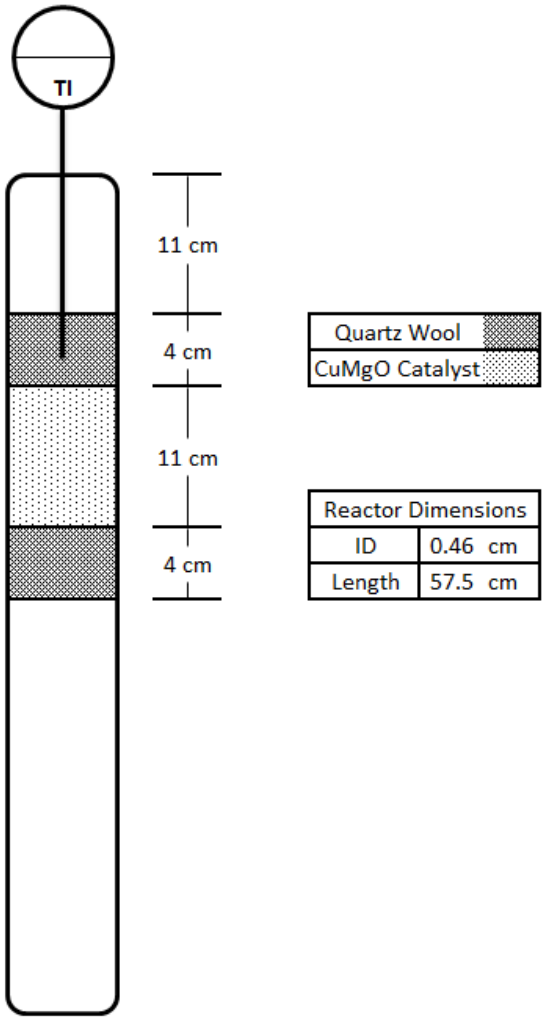

Figure 5: Reactor bed packing for reaction 2 with 1.0 gram catalyst and 0.063 gram quartz wool above and below catalyst

Above is an example of a catalyst packing (reaction 2) of the reactor bed, where 0.063 gram quartz wool was packed above and below 1.0 gram of Cu/MgO. Based on the weight of catalyst, the depth of the packing, and the cross sectional area of the reactor tube, the density of the catalyst was calculated to be about 590 kg/m^3 (see Table A-2).

Gas Chromatograph-Flame Ionized Detector (GC-FID)

GC-FID is a combined analytical tool that is very effective for identifying relative amounts of known compounds in a sample. The GC is a Thermo Scientific Trace GC Ultra with an attached Thermo Scientific Autosampler. It was essential to dilute the samples in an appropriate solvent, so that the analyzed compounds were placed on the column in the column's and FID's detectable range, which is on the magnitude of 10 ng. For the dilutions of the furfural and furfural hydrogenation products, ethyl acetate was chosen as it is a widely used solvent for GC-FID analysis and it has a much lower molecular weight than furfural or FA and as such a much faster retention time on the column. The GC-FID's autosampler allows the analysis to be run based on a user-defined sequence, which was created in triplicate with samples to examine repeatability. The major factors that affect a compounds retention time are its molecular weight, volatility, and its solubility with the film of the column. A Parker Balston Hydrogen Generator hydrolyses water to feed H_2 to the FID. The flame intensity of the flame ionized detector is based on the number of carbon atoms present in the compound, that said oxygen has a cancelling effect on the flame intensity, and as such an effective carbon number theory was created, which can also aid in determining relative sensitivities of compounds to the FID.[19]

A standard was created by pipetting 0.02 mL each of furfural and FA into a 100 mL volumetric flask with the balance filled with ethyl acetate. The autosampler then drew and injected 0.001 mL of the standard into the septum to the column. A split fraction of 100 was used, where He passes through at 100 mL/min, which further dilutes the sample so that 2.32 and 2.26 ng furfural and FA were injected to the column,

respectively. The retention times were then observed with furfural exiting the column after 22.06 minutes and FA exiting after 23.06 minutes. The Xcalibur program, which is the user interface attached to the GC-FID, can then be used to integrate for the areas under these peaks, and because equal amounts of furfural and FA were added it was necessary to normalize the peaks because of the FIDs sensitivity difference between the analyzed compounds; equal amounts of FA and furfural would lead to larger FA peaks. These sensitivities can be calculated on both a mass and molar basis based on equations 3 and 4.[19]

$$F_{mass} = \frac{area\ counts\ for\ reference. * weight\ of\ component}{area\ counts\ for\ component\ * weight\ of\ reference} \qquad (7)$$

Where:

F_{mass} = relative mass sensitivity of furfural to FA
area counts for reference = integrated peak area for furfural
weight of component = injection mass of FA (ng)
area counts for component = integrated peak area for FA
weight of reference = injection mass of furfural (ng)

$$F_{mole} = F_{mass} * \frac{MW\ of\ reference}{MW\ of\ component} \qquad (8)$$

Where:

F_{mole} = relative mole sensitivity of furfural to FA
F_{mass} = relative mass sensitivity of furfural to FA
MW of reference = molecular weight of furfural (g/mol)
MW of component = molecular weight of FA (g/mol)

The relative mass sensitivity and relative molar sensitivity of furfural to FA fluctuated from one GC-FID run to another, but the standards were always run twice per sequence and stayed in the 0.7 to 0.75 range.

Sample dilutions for the GC-FID were carried out by pipetting a 0.025 mL sample with Drummond Scientific Company Wiretrol II disposable pipets into a 10 mL

volumetric flask filled with ethyl acetate, this solution was mixed and then poured into a small beaker where 1 mL could be pipetted with a Fisherbrand 0.2-1.0 mL Finnpipette II into a second 10 mL volumetric flask with ethyl acetate. This solution was then poured into a 3 mL Luer-Lok tip Syringe and filtered through a Fisherbrand PTFE $4.5*10^{-4}$ mm filter to ensure no catalyst particles dirtied the sample, which could be harmful on the column of the GC-FID. All this corresponded to a dilution factor of 4000 (see Table A-3).

6. EXPERIMENT PLAN

The foundation of this research begins with the replication of N&R's results with their co-precipitated 16% copper loading on their Cu/MgO catalyst with conversion of 98% and selectivity of 98% to FA. The plan was to conduct selective vapor phase hydrogenation of furfural to FA under the same operating conditions, 15psi H_2, 1.2 mL/hr furfural, H_2/furfural ratio of 2.5, gas hourly space velocity (GHSV) of 0.05 mol/(hr*g catalyst), and 180°C. Once able to reproduce their results, the plan was to investigate reaction rate and catalyst performance over time.

As stated in N&R's work examining copper loadings they found 16% copper loading by weight to be optimal for both conversion of furfural and selectivity towards FA. This copper loading also corresponded to the highest BET-surface area. A similar surface area was calculated for the catalyst prepared for this work, as well.

Each reaction began with packing the catalyst between two plugs of quartz wool. Once the reactor was fitted into place, the system was pressure tested to a pressure of at least 40 psi, and fittings were adjusted accordingly until pressure was maintained

constant for 15-30 minutes. Then the system was left overnight to further ensure pressure was maintained.

Once the system passed the overnight pressure test the reactor was wrapped with heat tape and heated to 250°C with a H_2 flow rate of 15 standard cubic centimeters per minute (SCCM) and 15 psi for 4 hours. This process reduced the catalyst when the H_2 reacts with the CuO to produce Cu^0, which is the critical copper site for the selective reaction of furfural to FA.

After the 4 hours of reduction, the temperature controller was turned off while the H_2 flow and pressure were maintained. After the heat tape and reactor cooled enough to handle, 15-30 minutes, the heat tape was rewrapped to cover the furfural inlet to the reactor, as well as the fittings above the reactor tube to ensure that the furfural vaporized and stayed vaporized before passing through the catalyst bed. The system was then insulated and heated to 180°C for 45-60 minutes to ensure the system was at temperature before pumping furfural with a H_2 flow rate of 8.2 SCCM (H_2/furfural molar ratio of 2.5). The first two reactions were run with a H_2 flow rate of 8.2 SCCM, which was the calculated flow to keep the GSHV at 0.05 mol/(hr*g catalyst) with a H_2/furfural ratio of 2.5, but with a flow that low it was difficult to confirm H_2 flow through the rotameter. For that reason, reactions 3-6 were conducted with excess H_2 at 15 SCCM. The initial three reactions were run with 1 gram of catalyst with a focus on the first 5 hours with the objective of matching N&R's furfural conversion of 98% and FA selectivity of 98% over the first 5 hours of reaction time.

Once their results were matched or my results were at least repeatable, the plan was to investigate longer reactions to see how the catalyst performed over time. Also, to

lower the catalyst amount and/or increase the furfural flow to lower the conversion, and thus further investigate the catalyst performance and calculate the reaction rate. Also of interest was reusability of the catalyst.

7. DISCUSSION OF RESULTS

BET-Surface Area & Pore Size Distribution

The Micromeritics ASAP 2020 calculated a BET-Surface Area of 49.7 m^2/gm and the below figure shows how this surface area calculation compares to the results of N&R.

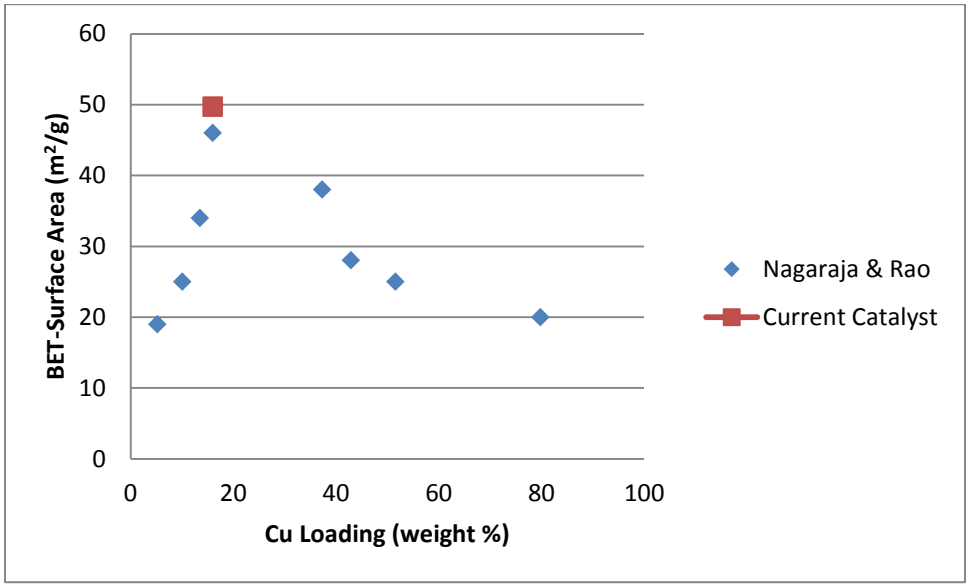

Figure 6: Plot comparing the surface area of the current catalyst in this study to those of N&R. Note that Cu loading for the current study was estimated based on the synthesis procedure, while the Cu loading for N&R was measured by Atomic Absorption Spectroscopy (AAS)

N&R calculated a BET-surface area of 46 m^2/g for their 16% Cu loaded catalyst (see Figure 6). This comparison is a decent indication that the current co-precipitated catalyst had a similar Cu loading. Considering their next Cu loading was 37.3%, it is possible the BET-surface area rises for increased loading of Cu after 16%, but there is no definitive claim to be made from this data.

Next, it is of interest to examine the isotherm of the volume of N_2 absorbed and desorbed as influenced by the relative pressure. The main area of interest on this plot (see Figure 7) is the linear region of low relative pressure between 0.05 and 0.2, and it is from values in this region that the BET-surface area is calculated. It is also of note to observe that the desorption curve lies below the adsorption curve in the relative pressure range of 0.75 to 1. This indicates the catalyst probably has mesopores as the N_2 gas more readily desorbs than adsorbs at any given equilibrium pressure in this range. N&R calculated an average pore size for their catalyst to be 2060 Angstrom,[17] which would actually be considered macropores, though N&R did not clearly state which synthesis method was used for that catalyst. Porosity diameter classifications are as follows, micropores up to 20 Angstrom, mesopores between 20-500 Angstrom, and macropores above 500 Angstrom.[18]

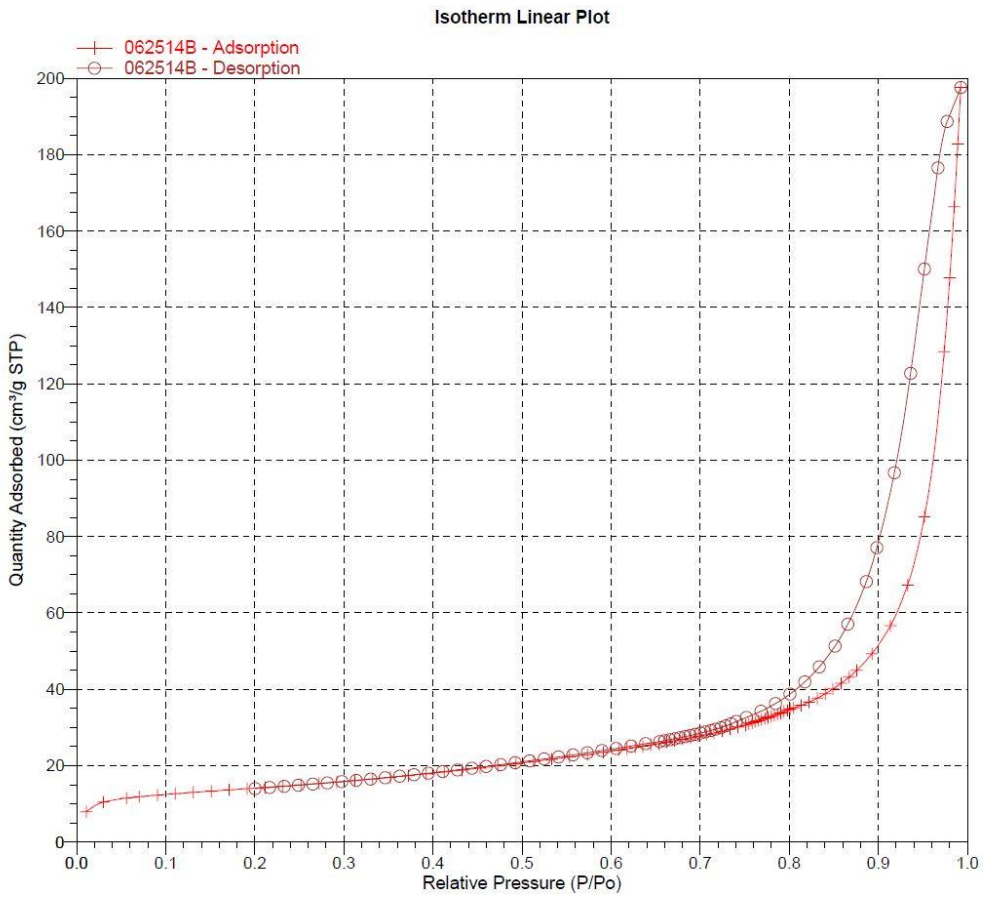

Figure 7: Plot of N_2 absorption and desorption in response to relative N_2 pressure, note that the difference between the absorption and desorption between relative pressures of 0.75 to 1 indicates mesopores, pores of at least 20 Angstrom

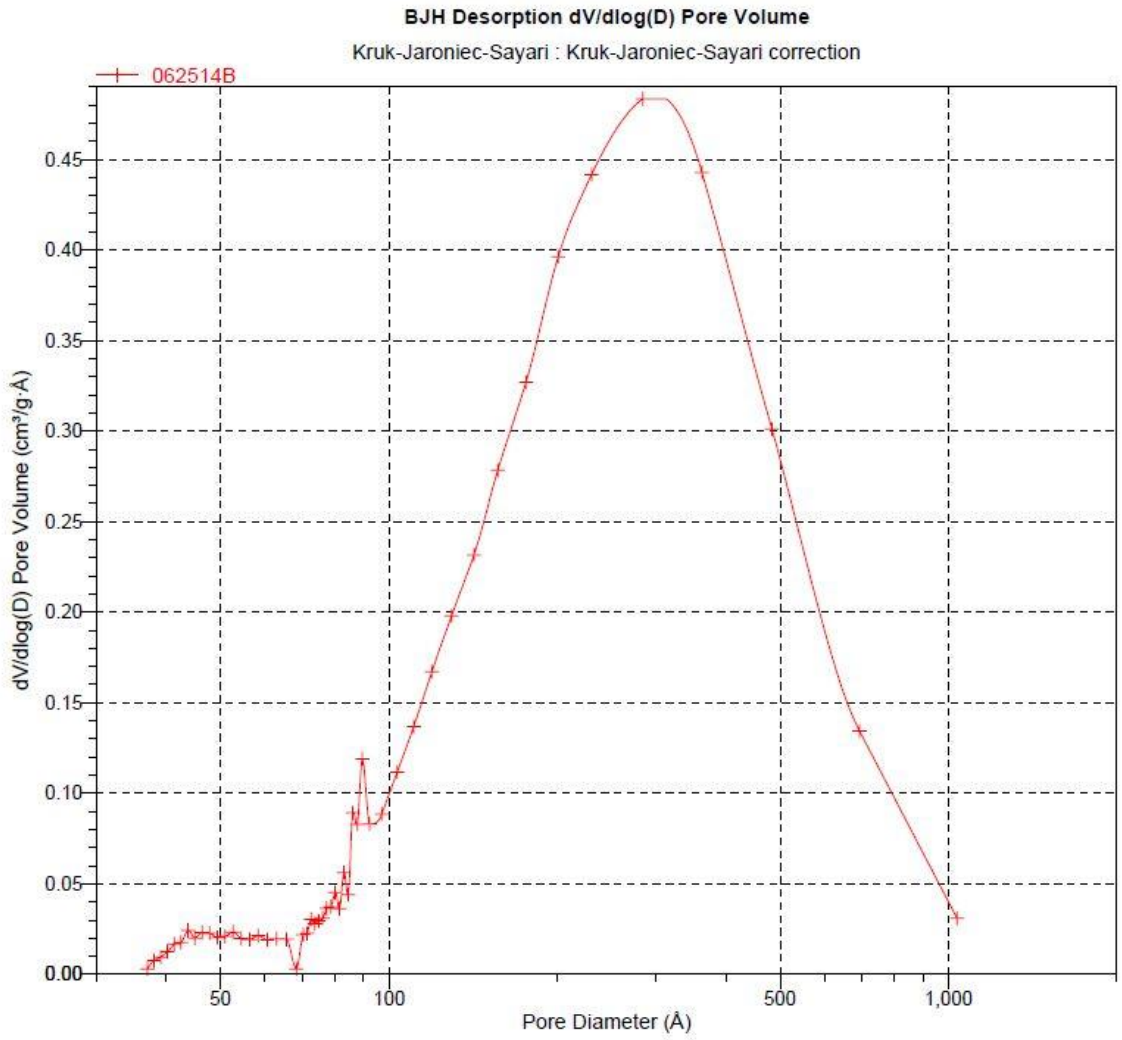

Figure 8: Plot of estimated pore size distribution based on N_2 adsorption and desorption differences with a most common pore size of about 300 Angstrom

As can be seen in Figure 8, above, the majority of the pore sizes are between 100 and 800 Angstrom in diameter with the most common pore diameter of about 300 Angstrom. These pore sizes are classified as mesopores and are nearly 7 times smaller in diameter than the catalyst of N&R.

Replication

The first several reactions run were designed to replicate N&R's results of 98% both for furfural conversion and selectivity towards FA. Their paper was not explicitly

clear whether these values were constant, averages, or maximums over the course of their five hour experiment. My goal was to replicate their data at five hours.

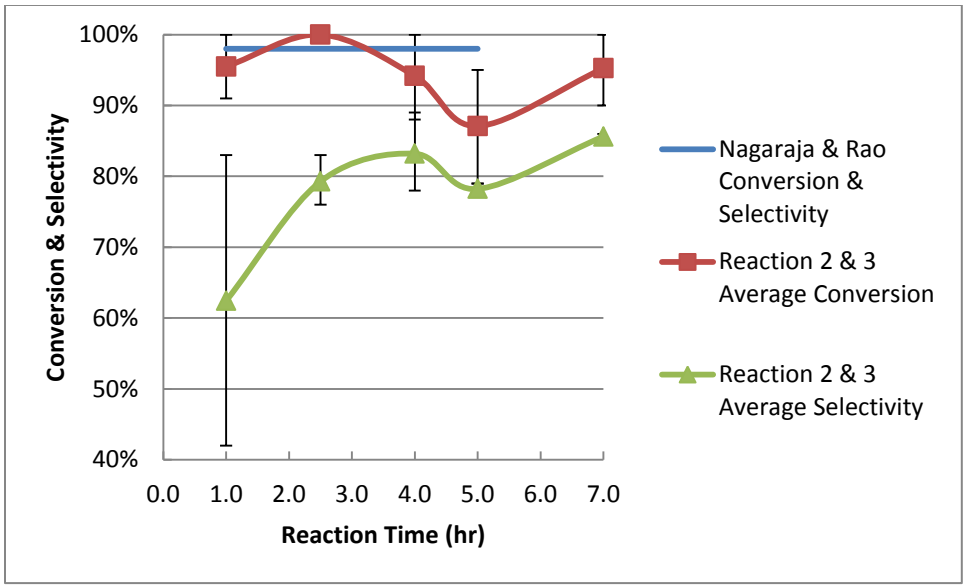

Figure 9: Plot examining reproducibility calculated conversion and selectivity, while comparing to N&R results (plotted as a flat line across the 5 hours experiment, but note it was not clear if these were averages, maximums or values after 5 hours), also note the error bars are the range of conversion and selectivity for reactions 2 & 3

I conducted two experiments at exactly the same operating conditions as N&R, and for the third experiment I increased the H_2 flow to 15 SCCM H_2 due to difficulty verifying H_2 flow on the rotameter at such a low H_2 flow rate. The first experiment saw fairly sporadic results with initially very low selectivity to FA and a steady drop off in furfural conversion from the 4^{th} to 7^{th} hours of the reaction (see Table A-4). Figure 9, above, shows the average furfural conversion and FA selectivity for the 2^{nd} and 3^{rd} reactions. The selectivity fell well short of N&R's results, but stayed fairly constant just below 80%, while the conversion was much closer to N&R's posted results with a fairly steady and average conversion of 94%, see Tables A-5 and A-6 for exact numbers on these reactions in the Appendix. Though these results did not perfectly match N&R, they did provide confidence towards the ability and reproducibility of the Cu/MgO catalyst to promote fairly high selectivity to FA and conversion of furfural.

Performance over Time

Reaction 4

With a decent idea of how the current co-precipitated catalyst performed in comparison with N&R, the next step was to examine how the catalyst performed over longer amounts of time to determine its appropriateness as a heterogeneous catalyst for continuous furfural hydrogenation to FA. The 4th reaction was conducted again at 180°C, with excess H_2 at 15 SCCM at 15 psi. The only difference with this reaction was that this time only 0.499 gram Cu/MgO was added to the reactor tube, but still surrounded by quartz wool. The objective of this reaction was to observe a steady furfural conversion in the region of 10-50% to calculate the reaction rate and assess the performance of the catalyst.

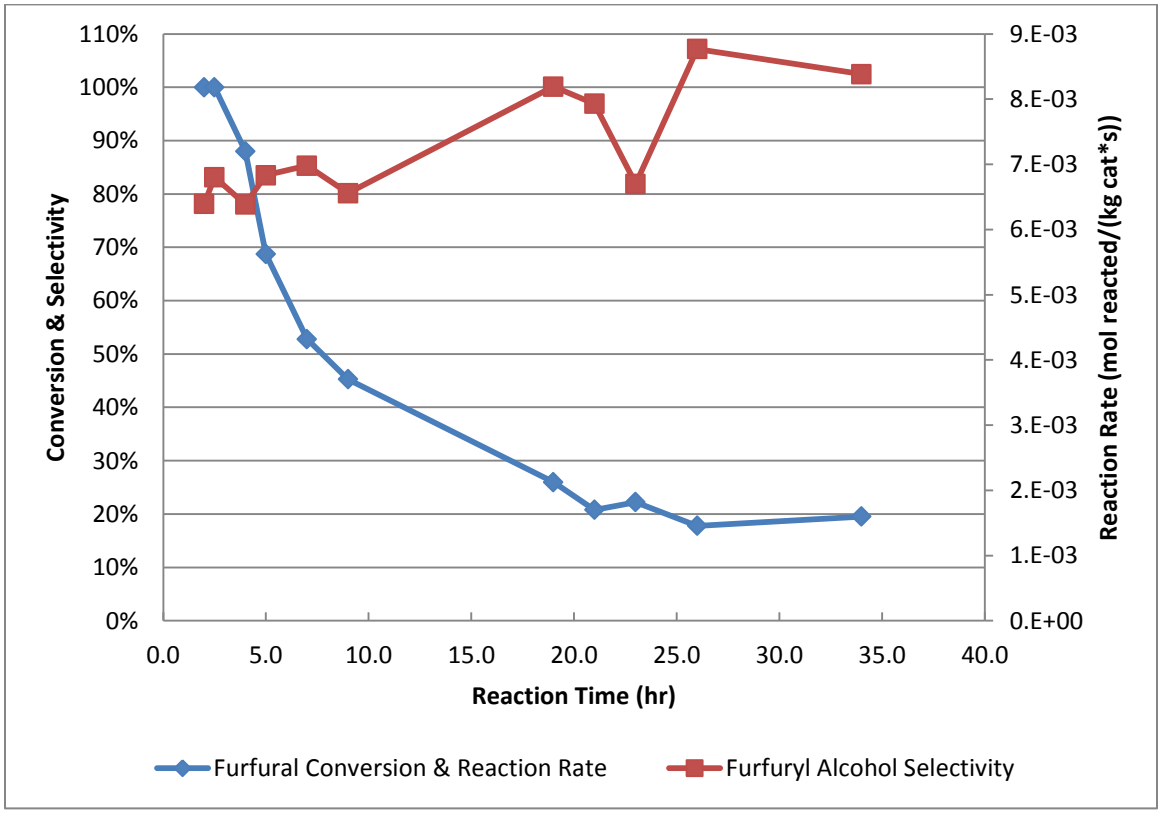

Figure 10: Plot of furfural conversion & FA Selectivity and reaction rate for reaction 4 with 0.499 g Cu/MgO at 180°C, with excess H2 at 15 SCCM at 15 psi

Figure 10, above, illustrates how conversion fell with time, but steadied off at about 20% 20 hours into the experiment, whereas the FA selectivity actually rose above the fairly consistent 80% seen thus far. The selectivity even rose above 100% for R4-10 and R4-11, but this is not possible. This stems from the GC-FID analysis and is likely an indicator that the furfural area was over calculated, thus indicating less furfural had reacted to produce the given amount of FA. The peaks for FA tended to be very symmetrical and straight forward to integrate, whereas the furfural peaks tended to tail off to the right, and as such a consistent determination of where to place the right end of the peak was difficult, but a systematic width of 0.08 minute was utilized.

Reaction rates were calculated (see Figure 10) with an emphasis on R4-8, R4-9, and R4-10, which correspond to the three samples taken 21, 23, and 26 hours into the experiment, respectively, which was where this steady state conversion of 20% occurred. The average reaction rate over that time period based on moles furfural reacted was $1.634*10^{-3}$ mol/(kg_{cat}*s) , The last sample, R4-11 was not included for this calculation because the reactor plugged at some point between R4-10 and R4-11, but the exact time of plugging was not known.

Some of the furfural was reacting to form other products, which is evident due to the FA selectivity that is less than 100%. Some of the most likely side products are 2-methylfuran, furan, tetrahydrofuran, and tetrahydrofurfuryl alcohol, but the main focus of this experiment was quantifying the selectivity towards FA versus towards each potential product. That said, it was of interest to examine how much of the sample composition was accounted for via the GC-FID analysis. In Figure 11, below, it can be seen that for the first 9 hours of the experiment the percent composition of each sample that was

identifiable rose from below 80 to above 90%, before being nearly entirely accounted for after 19 hours through to the end of the reaction. It is possible that some of this unknown percentage is unaccounted for furfural due to small peak to noise ratios or unidentified side products, such those listed above or tars in the catalyst bed. This coupled with the steady furfural conversion after 19 hours indicates it may have taken this reaction more than 10 hours to reach a steady state.

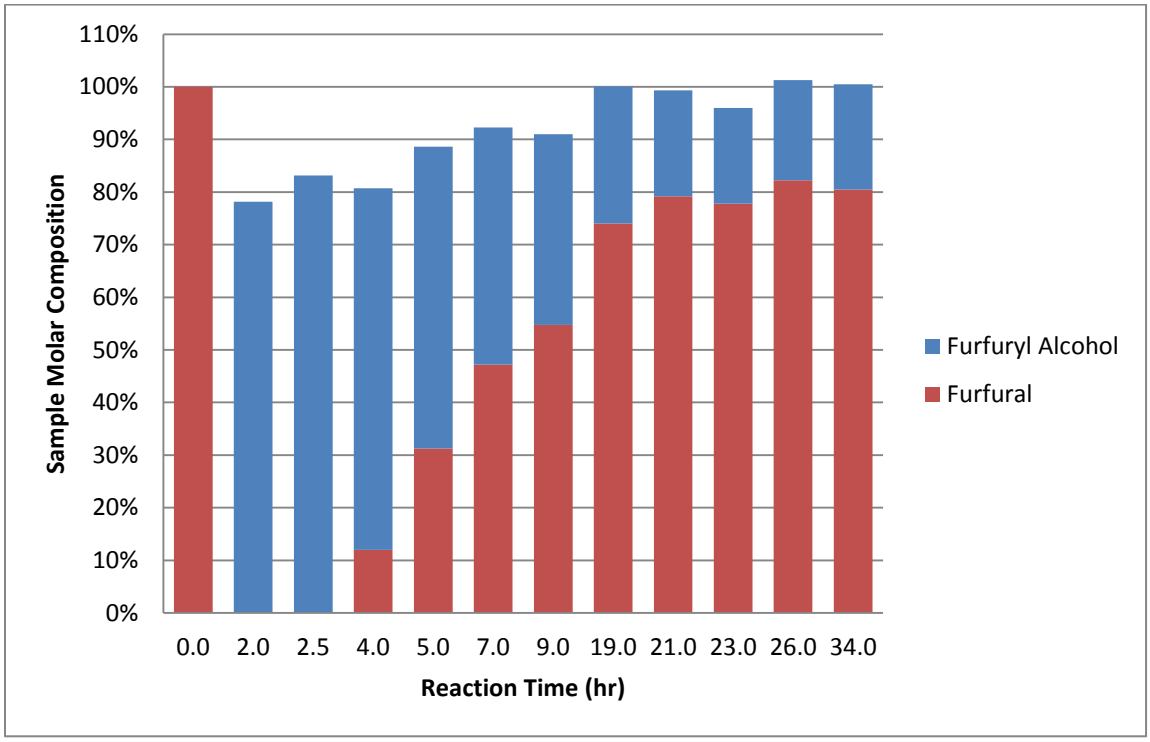

Figure 11: Molar composition balance for reaction 4 with 0.499 g Cu/MgO at 180°C, with excess H_2 at 15 SCCM at 15 psi, calculated based on feed molar area

Another form of analysis was to observe how the composition of samples combined with the mass collected for each sample. This was done by measuring the mass collected of each sample, multiplying these values by the mass compositions of furfural and FA for each sample, and then converting those masses into moles. This allows us to examine a molar flow balance below.

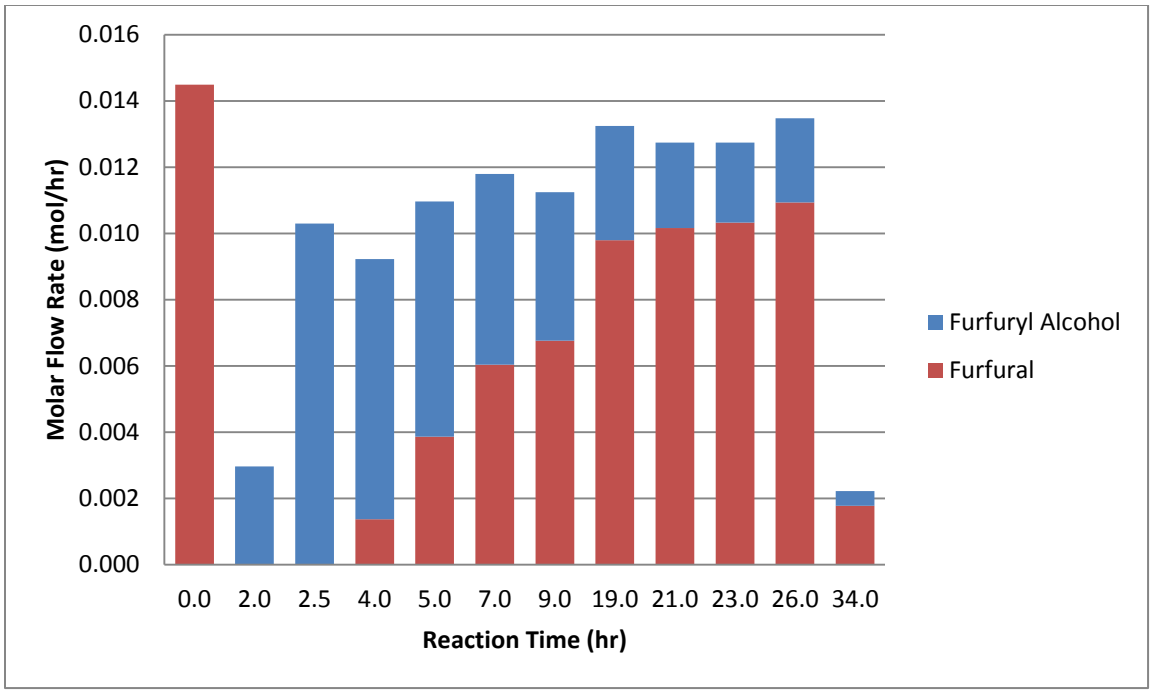

Figure 12: Molar flow balance for reaction 4 (0.499 g Cu/MgO at 180°C, with excess H_2 at 15 SCCM at 15 psi) as a comparison of the inlet flow rate of furfural and the known product composition and mass of product collected

An exact molar flow balance, based on the furfural to FA stoichiometry of 1:1, would have had the same molar flow rate coming out with any given sample collection as was fed via the HLPC pump, based on an hourly mole flow rate. That did not prove to be the case, but the majority of the molar flow could be accounted for between the 2.5 and 26.0 hour marks in the experiment (see Figure 12). Reasons these values may be low could be due to the potential unidentified side products of the hydrogenation reaction, missing small amounts from the collection vessel, minor inconsistencies in dilution method, and/or this could also be a result of error in the GC-FID area integration. It is likely that the 2 hour collection sample had such a low accounted for molar flow rate due to the system requiring time to reach steady state as furfural was slowly pumped through the system. The sample at 34 hours is low due to the aforementioned plugging of the reactor which occurred not too long after the sample was collected 26 hours into the experiment.

Another means for examining steady state operation of the reactor is to look at the mass balance over time. A cumulative mass balance percentage accounted for can be seen below in Figure 13. As seen in this figure it takes nearly 20 hours before the accounted for mass percentage levels of near 85%. Potential reasons for such low accounted for mass percentage over the first 10 hours could be due to hold up in the catalyst bed, the time it takes initially for the inlet furfural tube to fill with liquid furfural before it vaporizes, or the formation of non-condensable products or tars on the surface of the catalyst. The latter of these possibilities would be the most problematic and may explain some of the issues faced in this research. First, a buildup of non-condensable products on the surface of the catalyst would block active sites, thus lowering the available active sites for the furfural to react and the furfural conversion. If these tars were formed early in the reaction, it would explain the why the furfural conversion was so high and the mass closure was so low. That said the formation of tars would mean that the calculated selectivity to FA was inflated as these tars were not factored in the FA selectivity equation (see Sample Calculations B-3). If these non-condensable products and or tars continue to form eventually they will plug the catalyst bed, and these undesired products could be what made the reactor very difficult to clean after reaction 4 and 5.

Another issue to consider when trying to explain why the mass balance did not close is that of human error. Inefficiencies and human error in collecting from the collection vessel could have contributed to the lack of mass balance closure, but are unlikely major factors responsible for the lack of mass balance closure. When collecting from the collection vessel, the furfural and FA should have been cooled, based on their time in the room temperature collection vessel with no additional heat, so no vapor

should have escaped. The collection vessel was opened until a quick burst of vapor could be heard before being immediately closed, and it is possible some of that escaping gas was product. Also, after most collections there would typically be a drop or two of product that would fall from the vessel 15 to 30 seconds after the vessel was closed. These singular drops were occasionally missed, but it is improbable they would have had a major effect on the mass closure. Further data on the mass balance of the system can be seen in Table A-7.

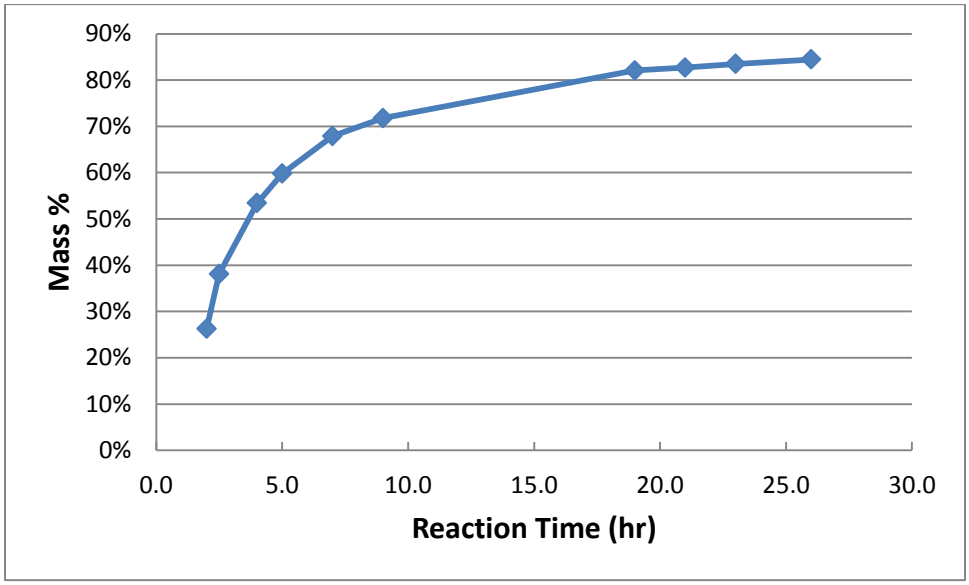

Figure 13: Cumulative mass percentage accounted for over time for reaction 4 determined by dividing mass of collected sample by mass flow rate set point times collection time; note this calculation does not consider the addition of H_2

After 5 hours of the experiment, the mass closure for reaction 4 was at 60% with 4.16 grams accounted for of the 6.96 grams expected to be collected. That is 2.8 grams unaccounted for over the first 5 hours of the experiment. N&R had no statement on mass closure in their results, so there is no comparison to be made with their research here.

Reaction 5

The reactor plugging was a significant issue, and the first attempt to prevent this from happening was to mix equal parts sand and catalyst before packing into the reactor bed. For reaction 5, I packed 0.5 gram catalyst with 0.503 gram sand to disperse the catalyst in an attempt to prevent potential decomposition. This actually led to the reactor bed plugging faster, roughly 21 hours into the experiment. FA selectivity stayed fairly constant with a few exceptions over the course of this reaction at about 0.75, while furfural conversion was still declining with time, which can be seen in Figure 14, below.

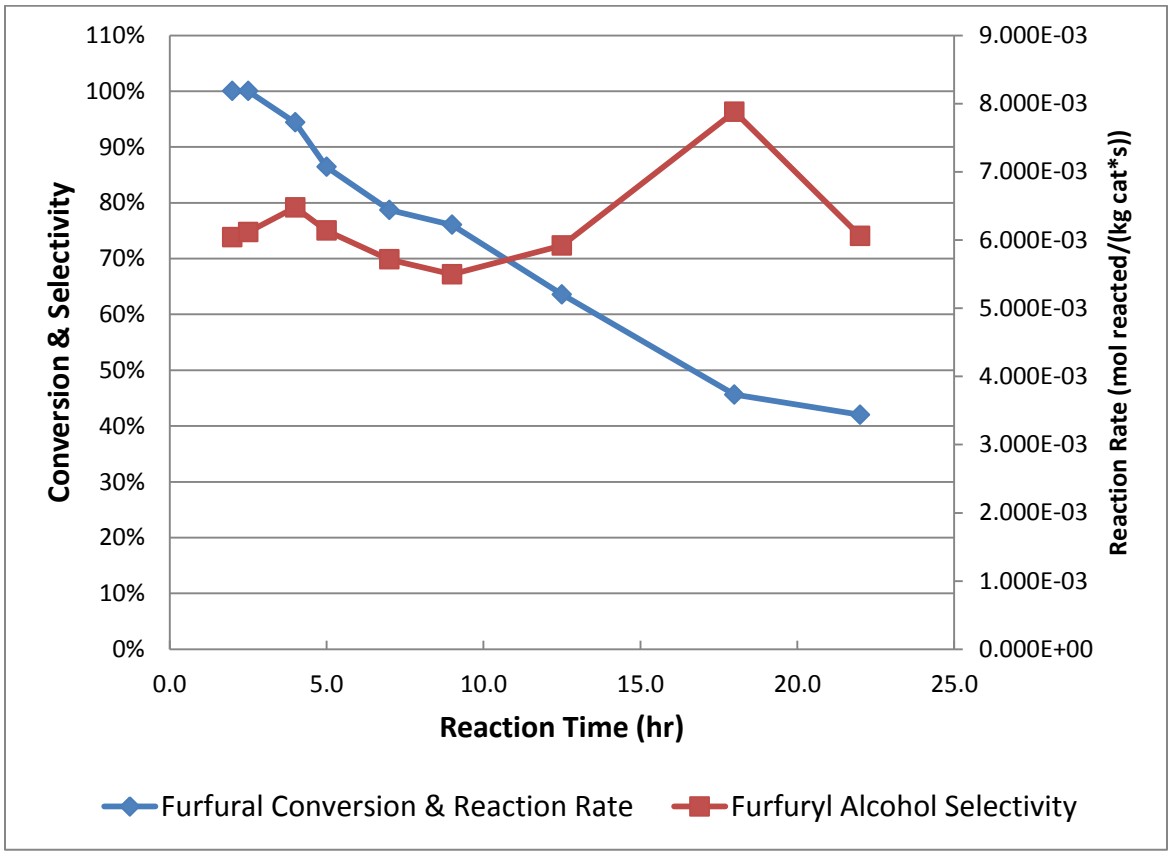

Figure 14: Plot of furfural conversion, FA Selectivity, & reaction rate for reaction 5 with 0.500 g Cu/MgO and 0.503 g sand at 180°C, with excess H2 at 15 SCCM at 15 psi

This continued decline indicates that the system was not able to reach steady state before plugging, but it is also interesting that with the equal mass sand to catalyst, at just past 20 hours the furfural conversion was near 40% versus near 20% without sand in reaction 4.

Though this reaction did not reach steady state, the reaction rates were still calculated and observed. Unsurprisingly, the reaction rates for reaction 5 (see Figure 14) were higher than reaction 4 due to the higher furfural conversion at comparative reaction times.

Further indication that steady state had not yet been reached can be seen in the molar composition balance below (see Figure 15). The percent molar composition of furfural was still on the rise when the reactor plugged, and the overall accounted for composition was rising, as well, over the last three samples collected.

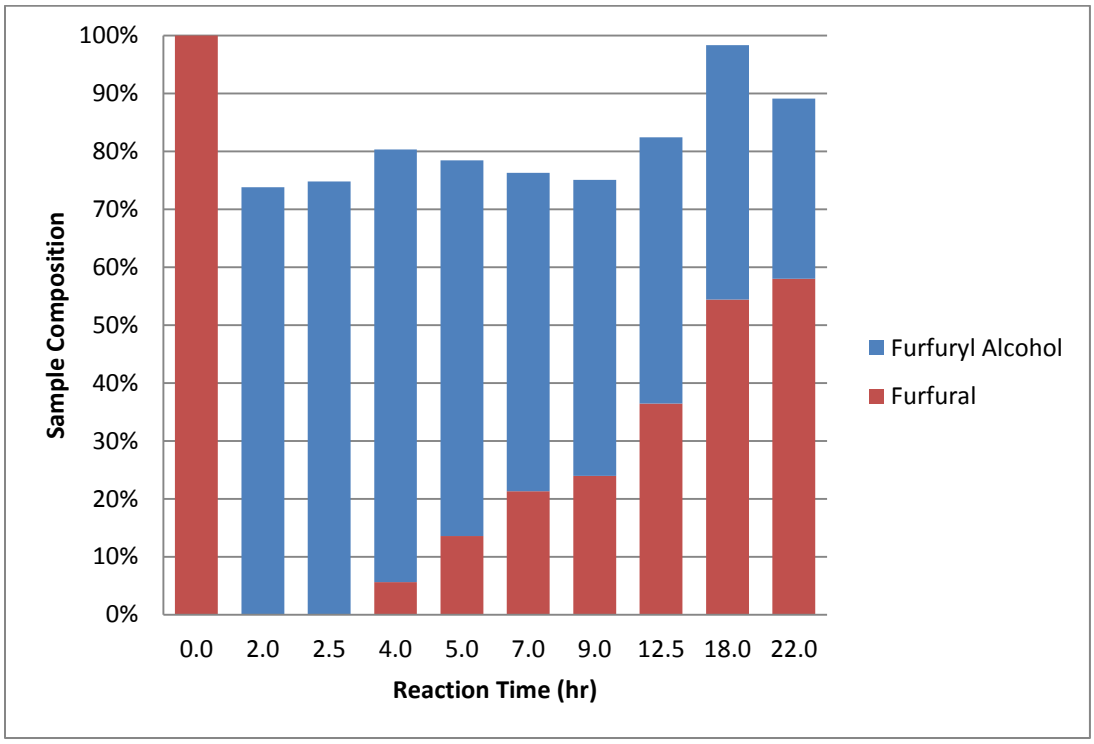

Figure 15: Molar composition balance for reaction 5 with 0.500 g Cu/MgO and 0.503 g sand at 180°C, with excess H_2 at 15 SCCM at 15 psi, calculated based on feed molar area

Though this reaction did not reach steady state, it is still of interest to examine the mass balance closure of the system (see Figure 16). The cumulative mass balance over time exhibited a very similar trend to reaction 4 with poor mass closure for the first ten hours before leveling off near 80% (see Table A-8). After 5 hours of the experiment, the

mass closure for reaction 5 was at 55% with 3.82 grams accounted for of the 6.96 expected to be collected. That is 3.14 grams unaccounted for over the first 5 hours of the experiment.

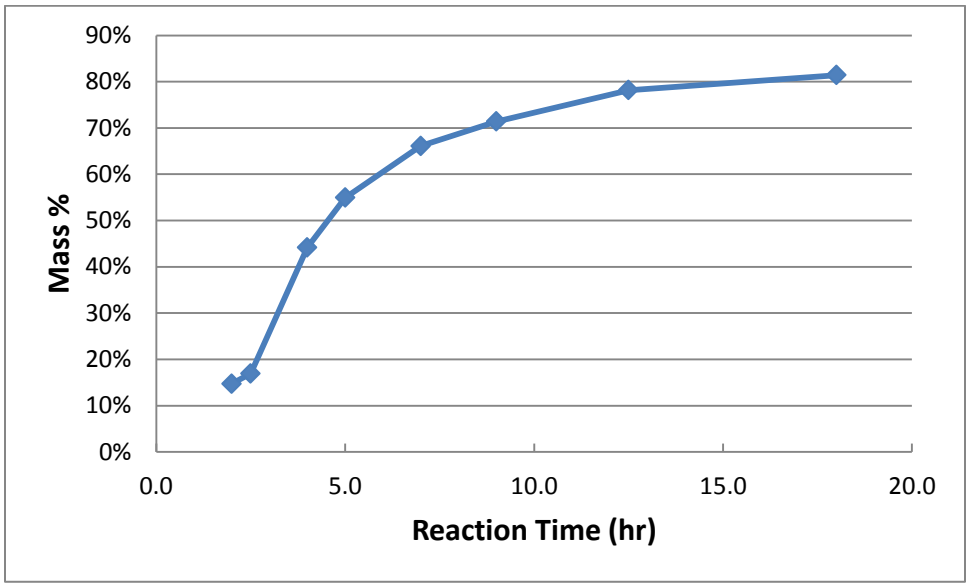

Figure 16: Cumulative mass percentage accounted for over time for reaction 5 determined by dividing mass of collected sample by mass flow rate set point times collection time; note this calculation does not consider the addition of H_2

Plugging of Reactor Tube

The most challenging cleanings of the reactor tube occurred after reactions 4 and 5 where the reactor plugged. It usually took about 30 minutes to clean the reactor tube, but after these runs it took over 2 hours of meticulously scraping out the stuck remnants of quartz wool, tarry catalyst, and metallic flaky solid fragments that could even be found up in the fittings above the reactor tube. Several of these factors seemed to hint that the furfural may be either polymerizing or decomposing, while being fed through the reactor tube, possibly because the reactor fittings had become too hot, but the thermal decomposition temperature, without the presence of oxygen, is 230°C[20], and it is improbable the reactor reached that high of temperature. In an attempt to isolate this issue and discover if the catalyst or furfural has been causing the problem, a 6th reaction was

conducted with 0.5 grams sand packed between quartz wool, while furfural was pumped at the same conditions as reactions 4 and 5 (1.2mL/hr, 180°C, 15SCCM H_2, and 15 psi H_2).

Reaction 6

This reaction ended up running 50.5 hours with no plugging of the reactor, which indicates that the furfural is likely not the issue with the plugging of the reactor bed. This further supports the hypothesis that there may be side products such as tars or non-condensable products forming in the Cu/MgO catalyst bed, which are responsible for the plugging of the reactor. The reaction 6 samples were run through the GC-FID and there was no appreciable conversion of furfural and no noticeable peaks to indicate any product was being formed.

8. CONCLUSION

This investigation into the performance of the co-precipitated Cu/MgO catalyst supports N&R's findings that this catalyst has great potential in terms of furfural conversion and FA selectivity over the first 5-10 hours of the reaction. That said, whether it is the catalyst, the furfural, or a reaction that occurs between the two that is responsible for the plugging of the reactor, there are certain hesitations to be had in regard to this catalytic experiment.

The major characterizations discovered for the current Cu/MgO catalyst:

- Cu/MgO has promise for selective hydrogenation of furfural to FA with furfural conversion of 94% and FA selectivity of 76% (averages for reactions 2 & 3)

- Reaction rate at approximately 20% conversion of $1.634*10^{-3}$ $mol/(kg_{cat}*s)$ based on moles furfural reacted (reaction 4)
- Reactor plugs after about 20-25 hours

Further effort should be placed to characterize the catalyst based on its elemental analysis to determine the exact Cu loading of the catalyst involved in this research. It would also be of interest to measure the Cu dispersion on the MgO to determine a turnover frequency. Beyond that a Thermal Gravitational Analysis should be conducted on the catalyst at 180°C for at least 30 hours to further understand if the catalyst has been responsible for the plugging of the reactor bed due to thermal decomposition. Furfural should, again, be run over a sand packed bed, without any catalyst, to see if furfural is repeatedly able to flow through the reactor without plugging it for at least 30 hours. Other areas of study would be to attempt conducting the reaction in the liquid phase by reducing the temperature and observing the effect on the furfural conversion and FA selectivity.

At this point I could not confidently suggest this catalyst for use in a continuous process due to the issues encountered with the reactor bed plugging, but the co-precipitated Cu/MgO catalyst was observed to perform well at these conditions for the first ten hours of any given reaction with at least 1.0 gram of catalyst (reactions 2 & 3).

Appendix A

Table A - 1: Co-precipitation Calculations for Desired 10 gram Cu/MgO

Weight Composition	0.16	Cu (wt%)	0.84	MgO (wt%)
Desired Amount (gm)	10	Gm		
Molar Composition	0.0252	mol Cu	0.208	mol MgO
	0.025	mol Cu-Nit	0.21	mol Mg-Nit
	6.08	gm Cu-Nit	53.44	gm Mg-Nit
Required Volume of 1 M	25.18	mL	208.41	mL

Table A - 2: Catalyst Density Calculations

Reaction	Catalyst Weight (gm)	Catalyst Height (cm)	Reactor Cross-Sectional Area (cm^3)	Catalyst Volume (cm^3)	Density (kg/m^3)
2	1.000	11	0.164	1.80	554
3	0.998	10	0.164	1.64	608
4	0.499	5	0.164	0.82	608
Average					**590**

Table A - 3: Sample Dilution Example

Sample Volume (mL)	Volume 1 Ethyl Acetate (mL)	Dilution Factor 1	Sample Volume 2 (mL)	Sample Volume 2 (mL)	Volume 2 Ethyl Acetate (mL)	Dilution Factor 2	Cumulative Dilution Factor
0.025	10	400	1	1	10	10	4000

Table A - 4: Reaction 1 Summary Results

Sample Notation	Reaction Sample Time(hr)	Furfural Conversion	FA Selectivity
Feed	0.0	-	-
R1-1	1.0	1.00	0.02
R1-2	2.5	1.00	0.63
R1-3	4.0	0.77	0.61
R1-4	5.0	0.74	0.82
R1-5	7.0	0.61	0.76

Table A - 5: Furfural Conversion Reproducibility

Sample Notation	Reaction Sample Time(hr)	Reaction 1	Reaction 2	Reaction 3	Average	Standard Deviation	Average 2 & 3
Feed	0.0	-	-	-	-	-	-
R#-1	1.0	1.00	0.91	1.00	0.97	0.05	0.95
R#-2	2.5	1.00	1.00	1.00	1.00	0.00	1.00
R#-3	4.0	0.77	1.00	0.88	0.89	0.11	0.94
R#-4	5.0	0.74	0.95	0.79	0.83	0.11	0.87
R#-5	7.0	0.61	1.00	0.90	0.84	0.20	0.95

Table A - 6: FA Selectivity Reproducibility

Sample Notation	Reaction Sample Time(hr)	Reaction 1	Reaction 2	Reaction 3	Average	Standard Deviation	Average 2 & 3
Feed	0.0	-	-	-	-	-	-
R#-1	1.0	0.02	0.42	0.83	0.42	0.40	0.62
R#-2	2.5	0.63	0.76	0.83	0.74	0.10	0.79
R#-3	4.0	0.61	0.89	0.78	0.76	0.14	0.83
R#-4	5.0	0.82	0.78	0.79	0.80	0.03	0.78
R#-5	7.0	0.76	0.86	0.85	0.82	0.05	0.86

Table A - 7: Reaction 4 Mass Balance Results

Reaction Sample Time (hr)	Cumulative Sample Collected Mass (g)	Cumulative Mass Flow Rate Setting (g)	% Cumulative Mass Accounted For	Cumulative Unaccounted Mass (g)	Unaccounted Mass (g)	Unaccounted Mass (g/hr)
0.0	-	-	-	-	-	-
2.0	0.73	2.78	0.26	2.05	2.05	1.03
2.5	1.33	3.48	0.38	2.16	0.10	0.20
4.0	2.97	5.57	0.53	2.60	0.44	0.29
5.0	4.16	6.96	0.60	2.80	0.20	0.20
7.0	6.62	9.74	0.68	3.13	0.33	0.16
9.0	8.99	12.53	0.72	3.54	0.41	0.21
19.0	21.71	26.45	0.82	4.74	1.20	0.12
21.0	24.17	29.23	0.83	5.06	0.32	0.16
23.0	26.73	32.02	0.83	5.29	0.23	0.12
26.0	30.56	36.19	0.84	5.63	0.34	0.11

Table A - 8: Reaction 5 Mass Balance Results

Reaction Sample Time (hr)	Cumulative Sample Collected Mass (g)	Cumulative Mass Flow Rate Setting (g)	% Cumulative Mass Accounted For	Cumulative Unaccounted Mass (g)	Unaccounted Mass (g)	Unaccounted Mass (g/hr)
0.0	-	-	-	-	-	-
2.0	0.41	2.78	0.15	2.37	2.37	1.19
2.5	0.59	3.48	0.17	2.89	0.52	1.03
4.0	2.46	5.57	0.44	3.11	0.22	0.15
5.0	3.82	6.96	0.55	3.14	0.03	0.03
7.0	6.44	9.74	0.66	3.30	0.17	0.08
9.0	8.94	12.53	0.71	3.59	0.28	0.14
12.5	13.60	17.40	0.78	3.80	0.22	0.06
18.0	20.40	25.06	0.81	4.66	0.85	0.16

Appendix B

Sample Calculation B - 1: Calculation of GC-FID mass and molar area count sensitivities

All of the following sample calculations were conducted from sample R4-6.

Molecular Weights: $MW_F := 96.08 \frac{gm}{mol}$ $MW_{FA} := 98.1 \frac{gm}{mol}$

GC-FID Sensitivity Correction Factor Calculated Using Standard with 20 uL each of Furfural and FA

Standard Areas: $AS_F := 133372$ $AS_{FA} := 183895$

Standard Mass to Column: $mass_F := 232ng$ $mass_{FA} := 226ng$

Dilution Factor: $DF := 5000$

Dilution Corrected Area: $AS_F := 133372 \cdot DF$ $AS_{FA} := 183895 \cdot DF$

Mass Sensitivity: $F_{mass} := \frac{AS_F \cdot mass_F}{AS_F \cdot mass_F} = 1$ $FA_{mass} := \frac{AS_F \cdot mass_{FA}}{AS_{FA} \cdot mass_F} = 0.707$

Molar Sensitivity: $F_{mol} := F_{mass} \cdot \frac{MW_F}{MW_F} = 1$ $FA_{mol} := FA_{mass} \cdot \frac{MW_F}{MW_{FA}} = 0.692$

Sample Calculation B - 2: Furfural fractional conversion (X_F)

Average of 3 Area Counts for Feed Furfural: $A_{F0} := 168492$

Average of 3 Area Counts: $A_F := 92207$ $A_{FA} := 87988$

Dilution Factor: $DF := 4000$

Dilution Corrected Area: $A_{F0} := A_{F0} \cdot DF = 6.74 \times 10^8$

$A_F := A_F \cdot DF = 3.688 \times 10^8$ $A_{FA} := A_{FA} \cdot DF = 3.52 \times 10^8$

Molar Sensitivity Correction: $A_F := A_F \cdot F_{mol} = 3.688 \times 10^8$ $A_{FA} := A_{FA} \cdot FA_{mol} = 2.435 \times 10^8$

Conversion: $X_F := \frac{A_{F0} - A_F}{A_{F0}} = 0.453$

Sample Calculation B - 3: Furfuryl alcohol selectivity (S_{FA})

$$S_{FA} := \frac{A_{FA}}{A_{F0} - A_F} = 0.798$$

Sample Calculation B - 4: Reaction rate based on furfural fractional conversion, flow rate fed to the reactor, and amount catalyst packed in reactor bed

HPLC Furfural Set Point: $V_F := 1.2\frac{mL}{hr}$

Furfural Density: $\rho_F := 1.16\frac{gm}{mL}$

Molar Flow Rate Furfural from HPLC Pump: $F_{F0} := V_F \cdot \rho_F \cdot \frac{1}{MW_F} = 0.014\frac{mol}{hr}$

Mass Catalyst Packed in Reactor Bed: $mass_{cat} := 0.499gm$

Reaction Rate: $r_F := \frac{F_{F0} \cdot X_F}{mass_{cat}} = 3.651 \times 10^{-3}\frac{mol}{kg \cdot s}$

Sample Calculation B - 5: Cumulative mass accounted for after 9 hours of reaction based on mass of sample collected and set point of HPLC pump; note: this neglects influence of H_2 gas

Collected Mass Samples:

$mass_{RF1} := 0.73gm$ $mass_{RF2} := 0.595gm$ $mass_{RF3} := 1.648gm$

$mass_{RF4} := 1.188gm$ $mass_{RF5} := 2.456gm$ $mass_{RF6} := 2.374gm$

Cumulative Collected Mass After Collecting RF-6 (9 hours of reaction time):

$mass_{coll} := mass_{RF1} + mass_{RF2} + mass_{RF3} + mass_{RF4} + mass_{RF5} + mass_{RF6} = 8.991\,gm$

Furfural Mass Pumped From HPLC PUMP (Based on Set Point):

$mass_{fed} := V_{F0} \cdot \rho_F \cdot 9hr = 12.528\,gm$

Cumulative Mass Accounted For at R4-6:

$mass_{per} := \frac{mass_{coll}}{mass_{fed}} = 0.718$

References

1 K. Yan, G. Wu, T. Lafleur and C. Jarvis. Production, properties and catalytic hydrogenation of furfural to fuel additives and value-added chemicals. *Renewable and Sustainable Energy Reviews* 2014; **38**; 663-676.

2 D. J. Hayes, S. Fitzpatrick, M. H. B. Hayes and J. R. H. Ross. Biofine process – production of levulinic acid, furfural, and formic acid fromlignocellulosic feedstocks. *Biorefineries Industrial Processes and Products* 2006; ed. B. Kamm, P. R. Gruber and M. Kamm, **1**,139–164.

3 J.J. Bozell and G.R. Petersen. Technology development for the production of biobased products from biorefinery carbohydrates—the US Department of Energy's "Top 10" revisited. *Green Chem.* 2010; **12**; 539-534.

4 J.N. Chheda, Y. Román-Leshkov and J.A. Dumesic. Production of 5-hydroxymethylfurfural and furfural by dehydration of biomass-derived mono- and poly-sachharides. *Green Chem.* 2007; **9**; 342-350.

5 W.S. Lee, Z. Wang, W. Zheng, D.G. Vlachos and A. Bhan. Vapor phase hydrodeoxygenation of furfural to 2-methylfuran on molybdenum carbide catalysts. *Catal. Sci. Technol.* 2014; **4**; 2340-2352.

6 D.F. Aycock. Solvent applications of 2-methyltetrahydrofuran in organometallic and biphasic reactions. Org. Process Res. Dev. 2007; **11**; 156-159.

7 G.W. Huber, S. Iborra, and A. Corma. Sythesis of transportation fuels from biomass: chemistry, catalysts, and engineering. Chem Rev. 2006; **106**; 4044-4098.

8 P. Lejemble, A. Gaset, and P. Kalck. From biomass to furan through decarbonylation of furfural under mild conditions. *Biomass* 1984; **4**; 263-274.

9 M. Messori and A. Vaccari. Reaction pathway in vapor phase hydrogenation of maleic anhydride and its esters to γ-butryolactone. *Journal of Catalysis* 1994 ;**150**; 177-185.

10 J.G. Stevens, R.A. Bourne, M.V. Twigg and M. Poliakoff. Real-time product switching using a twin catalyst system for the hydrogenation of furfural in supercritical CO_2. *Angew. Chem. Int. Ed.* 2010; **49**; 8856-8859.

11 J.B. Barr and S.B. Wallon. The chemistry of furfuryl alcohol resins. *Journal of Applied Polymer Science* 1971; **15**; 1079-1090.

12 http://www.alibaba.com/product-detail/furfural_60126033865.html?s=p, accessed April 2015

13 http://www.alibaba.com/product-detail/high-quality-Furfuryl-Alcohol-CAS-98_60137506402.html?s=p, accessed April 2015

14 L. Zheng, Z. Huang, J. Liu and C. Xu. Furfural hydrogenation on nickel-promoted cu-containing catalysts prepared from hydrotalcite-like precursors. *Chin. J. Chem.* 2011; **29**; 691-697.

15 S. Sitthisa and D.E. Resasco. Hydrodeoxygenation of furfural over supported metal catalysts: a comparative study of Cu, Pd, and Ni. *Catal. Lett.* 2011; **141**; 784-791.

16 B.M. Nagaraja, A.H. Padmasri, B.D. Raju and K.S. Rao. Vapor phase selective hydrogenation of furfural to furfuryl alcohol over Cu-MgO co-precipitated catalysts. *Journal of Molecular Catalysis A: Chemical* 2007; **265**; 90-97.

17 B.M. Nagaraja, V.S. Kumar, V. Shasikala, A.H. Padmasri, B. Sreedhar, B.D. Raju and K.S. Rao. A highly efficient Cu/MgO catalyst for vapour phase hydrogenation of furfural to furfuryl alcohol. *Catalysis Communications* 2003; **4**; 287-293.
18 P.A. Webb and C. Orr. Analytical methods in fine particle technology. Norcross: Micromeritics. 1997. 301 p.
19 J.T. Scanlon and D.E. Willis. Calculation of flame ionization detector relative response factors using the effective carbon number concept. *Journal of Chromatographic Science* 1985; **23**; 333-340.
20 A.P. Dunlop and F.N. Peters Jr. Thermal stability of furfural. *Ind. Eng. Chem* 1940; ***32***; 1639–1641.

Author's Biography

Andrew is an avid fan of reading, writing, improvised acting, statistics, sports, hiking, and music. After graduation, Andrew will spend four months in Hawaii volunteering with the Hawaii Island Hawksbill Turtle Recovery Project. After completing his time with this project, Andrew plans to find work in the energy industry.